Energy & Environmental Science

REVIEW

Cite this: *Energy Environ. Sci.*, 2018, **11**, 276

Emerging electrochemical and membrane-based systems to convert low-grade heat to electricity

Mohammad Rahimi, [a] Anthony P. Straub, [b] Fang Zhang, [c] Xiuping Zhu, [d] Menachem Elimelech, [e] Christopher A. Gorski [f] and Bruce E. Logan *[f]

Received 21st October 2017,
Accepted 21st December 2017

DOI: 10.1039/c7ee03026f

rsc.li/ees

Low-grade heat from geothermal sources and industrial plants is a significant source of sustainable power that has great potential to be converted to electricity. The two main approaches that have been extensively investigated for converting low-grade heat to electrical energy, organic Rankine cycles and solid-state thermoelectrics, have not produced high power densities or been cost-effective for such applications. Newer, alternative liquid-based technologies are being developed that can be categorized by how the heat is used. Thermoelectrochemical cells (TECs), thermo-osmotic energy conversion (TOEC) systems, and thermally regenerative electrochemical cycles (TRECs) all use low-grade heat directly in a device that generates electricity. Other systems use heat sources to prepare solutions that are used in separate devices to produce electrical power. For example, low-temperature distillation methods can be used to produce solutions with large salinity differences to generate power using membrane-based systems, such as pressure-retarded osmosis (PRO) or reverse electrodialysis (RED); or highly concentrated ammonia solutions can be prepared for use in thermally regenerative batteries (TRBs). Among all these technologies, TRECs, TOEC, and TRBs show the most promise for effectively converting low-grade heat into electrical power mainly due to their high power productions and energy conversion efficiencies.

Broader context

Low-grade heat is a large untapped energy resource generated at various industrial plants and available from geothermal sources. Due to lack of efficient and cost-effective recovery methods, low-grade heat has generally been discarded by industry and has become an environmental concern because of thermal pollution. The critical needs for technologies that convert low-grade waste heat into electricity are a high power output, efficiency, scalability, and cost-effectiveness. Research into converting low-grade heat to electrical energy has previously focused on solid-state devices and organic Rankine cycles. The primary limitations of these approaches are their low power densities and high materials costs. Liquid-based electrochemical or membrane systems offer an alternative that is potentially cheaper and scalable. The main liquid-based technologies are thermoelectrochemical cells, thermo-osmotic energy conversion systems, thermally regenerative electrochemical cycles, salinity gradient energy based systems, and thermally regenerative batteries. Among these, the most favorable emerging technologies are thermo-osmotic energy conversion systems, thermally regenerative electrochemical cycles, and thermally regenerative batteries due to improved conversion efficiencies and higher power densities. In this article, we discuss these emerging as well as conventional liquid-based technologies and provide our perspective on the potential of low-grade heat conversion technologies for cost-effective electricity generation.

1. Introduction

Significant quantities of low-grade heat (temperature $<130\ ^{\circ}C$) are available globally from geothermal sources and various industrial plants.[1–4] The potential low-temperature energy from geothermal sources was estimated to be significantly higher than the annual global energy consumption including transportation.[5–7] Low-grade waste heat generated at industrial plants in the USA equals approximately half of the current energy demand of the United States (2.9×10^4 TW h in 2013) (Fig. 1).[8,9] The waste heat potential of primary energy sectors in China, the world's largest energy consumer, is estimated to range from 15% to 40% of the

[a] *Department of Chemical Engineering, The Pennsylvania State University, University Park, PA 16802, USA*
[b] *Department of Materials Science and Engineering, Massachusetts Institute of Technology, Cambridge, Massachusetts 02139, USA*
[c] *School of Environment and State Key Joint Laboratory of Environment Simulation and Pollution Control, Tsinghua University, Beijing, 100084, China*
[d] *Department of Civil and Environmental Engineering, Louisiana State University, Baton Rouge, LA 70803, USA*
[e] *Department of Chemical and Environmental Engineering, Yale University, New Haven, CT 06520, USA*
[f] *Department of Civil and Environmental Engineering, The Pennsylvania State University, University Park, PA 16802, USA. E-mail: blogan@psu.edu; Tel: +1 814 863 7908*

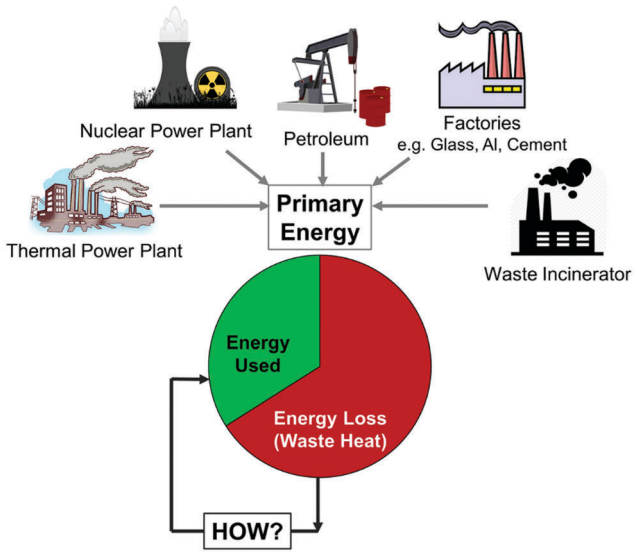

Fig. 1 Waste heat production in the primary industrial energy sectors.

total fuel input.[10] In the UK, the potential cost savings with low-grade waste heat recovery could reach $370 M per year, with potential greenhouse gas reductions of up to 2093 $ktCO_2$ eq. per year.[11]

Technologies to convert low-grade heat to electricity must produce high power densities (per unit area or volume) and be efficient, scalable, and cost-effective.[2,12] Among the different methods for converting low-grade heat into electricity, organic Rankine cycles (ORCs) and solid-state thermoelectrics (TEs), have been the most extensively studied.[1,13–17] An ORC is an engine that converts heat into mechanical work that is used to produce electrical power.[18–20] The organic working fluids for an ORC must have relatively low boiling points and high vapor pressures (*e.g.*, hydrochlorofluorocarbons or hydrocarbons) so that they can be evaporated using low-grade heat.[18,21,22] The working fluid in an ORC first evaporates and then expands in a conventional mechanical to electricity conversion system.[1,23] TEs offer a simpler approach based on direct conversion of temperature differences to electrical power using semiconductors or semi-metals that have high electrical conductivities and thermoelectric sensitivities (*i.e.*, Seebeck coefficients).[24–27] In a TE device, voltage is generated from different temperatures on each side of the device.[13,28] Despite much progress over the past decades, ORCs and TEs have not been used for large-scale conversion of low-grade heat to electricity for various reasons, including relatively low power densities, high material and/or operational costs, lack of capacities for energy storage, system complexity, and low heat-to-electricity conversion efficiencies.[29–31]

New, liquid-based technologies are an alternative approach for conversion of low-grade heat into electricity that may be more effective than past approaches.[32] These new technologies can be categorized into two major groups based on how the heat source is applied: direct and indirect utilization of low-grade heat. Thermoelectrochemical cells (TECs),[33] thermo-osmotic energy conversion (TOEC) devices,[34] and thermally regenerative electrochemical cycles (TRECs)[35] all use low-grade heat directly in a device that simultaneously generates electrical power. In indirect utilization, low-grade heat is used to produce solutions that have differences in salinities or concentrations, which are subsequently fed into a separate power production unit. The two main indirect methods of utilizing low-grade heat through external fluid regeneration that are being developed are salinity gradient energy (SGE) systems[36] and thermally regenerative batteries (TRBs).[37] We review here both groups of liquid-based methods, summarize their power densities together with their thermal-electrical efficiencies, and provide our perspective on the potential of these low-grade heat conversion technologies for cost-effective electricity generation.

2. Methods for direct conversion of low-grade heat to electricity

For direct electrical power generation from low-grade heat, the heat source is applied directly to the power production unit and therefore continuously generates electrical power from solutions with two different temperatures. With TECs and TOEC systems, different temperatures are applied to different sides of the cell, while in a TREC, the cell is charged and discharged at different temperatures.

2.1. Thermoelectrochemical cells

TECs produce steady electric current under an applied temperature difference between the electrodes. The hot electrode is designated as the anode, and the cold electrode as the cathode.[38–40] The cell that is filled with a temperature-dependent redox couple (*e.g.*, ferri/ferrocyanide) in an aqueous,[41,42] non-aqueous (*e.g.*, ionic liquid),[32,43] or mixed electrolyte[44,45] creates a potential difference proportional to its Seebeck coefficient. When the circuit is closed, current flows to reach electrochemical equilibrium. The reduced species are oxidized at the anode and generated at the cathode. The built-up concentration gradient drives a flux that returns the reduced species to the anode and the oxidized species to the cathode. A steady-state current is maintained as long as there is a temperature difference between the electrodes (Fig. 2).[31,46]

Since the introduction of a TEC in 1957,[47] the maximum power densities (P) and thermal-electrical conversion efficiencies, reported relative to Carnot efficiency ($\eta_{t/C}$), have significantly improved, especially by using carbon nanotube electrodes. For example, in 1996, a TEC with a ferri/ferrocyanide redox couple in an aqueous electrolyte and platinum electrodes produced only $P = 3.6 \times 10^{-3}$ W m^{-2}-electrode pair area with $\eta_{t/C} = 0.6\%$.[48] By 2010, these had been increased to $P = 1.8$ W m^{-2} and $\eta_{t/C} = 1.4\%$ using multi-walled carbon nanotube (MWCNT) buckypaper electrodes and the same redox couple.[31] The highest reported efficiency relative to the Carnot limit for a TEC is 3.95% (P = 6.6 W m^{-2}) based on using a carbon-nanotube aerogel-based electrode in an aqueous ferri/ferrocyanide electrolyte.[42] The highest power density of a TEC of 12 W m^{-2} was obtained by using a highly concentrated ferri/ferrocyanide electrolyte, but at a lower efficiency of $\eta_{t/C} = 0.4\%$.[49]

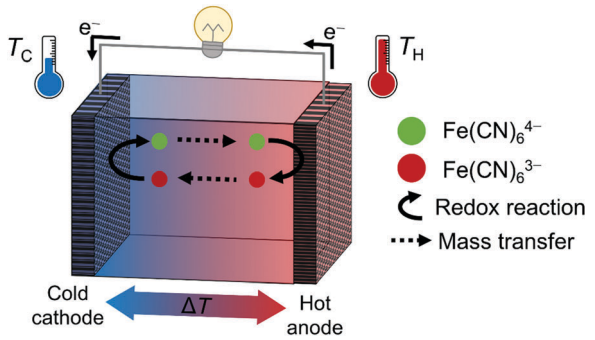

Fig. 2 Schematic of a TEC with a ferri/ferrocyanide redox couple. A steady-state current is maintained as long as there is a temperature difference between the electrodes.

2.2. Thermally regenerative electrochemical cycles

Electricity production based on the TREC method was originally developed a few decades ago for operation at high-temperatures (>500 °C), with the percentage of the Carnot efficiency reaching 40–50%. Through fabrication of electrode materials with a fast charge transfer and high charge capacity at low temperatures, a TREC operating at low temperatures (<130 °C) was demonstrated a few years ago.[35,50] TREC conversion of low-grade heat to electricity uses an electrochemical cell in which electrodes discharged at a low temperature (T_L) can be recharged at a higher temperature (T_H). The charging voltage at T_H is lower than the discharging voltage at T_L, which leads to net energy production by the voltage difference (Fig. 3).[35,51,52] The electrode materials used in TRECs include solid copper hexacyanoferrate (CuHCF) cathodes and Cu anodes,[35] nickel hexacyanoferrate (NiHCF) cathodes and Ag/AgCl anodes,[52] and Prussian blue particles on both carbon cloth electrodes.[51] The thermal-electrical efficiencies of these low temperature TRECs have been significantly higher than those of TECs. For example, a maximum thermal efficiency of 5.7% ($\eta_{t/C}$ = 38%) was obtained in a TREC with a CuHCF cathode and Cu anode, with the cell operated at a temperature difference of 50 °C (T_L of 10 °C and T_H of 60 °C). Sodium nitrate was used in the catholyte, while a copper nitrate was used in the anolyte, and an anion exchange membrane was used to separate the chambers and avoid the transfer of copper ions from the anolyte to the catholyte, which would produce an undesirable side reaction between CuHCF and copper ions.[35]

One potential issue with TRECs that use CuHCF and Cu electrodes is the need for an anion exchange membrane, which increases capital and maintenance costs and loses its perm-selectivity at higher temperatures.[53] To avoid these problems, the ion-selective membrane was replaced by an inexpensive porous separator. Using a NiHCF cathode and a silver/silver chloride anode with a glass fiber filter separator, and a potassium chloride and nickel nitrate electrolyte, a TREC achieved a maximum thermal efficiency of 3.5% ($\eta_{t/C}$ = 29%), when operating between 15 °C and 55 °C.[52] The system also showed a better cycling performance compared to the previous TREC with CuHCF/Cu electrodes.

While most TRECs require additional external electrical power for the charging process, one TREC was developed where the charging process was accomplished using thermal energy. The cell consisted of a carbon cloth electrode loaded with Prussian blue particles immersed in a soluble ferrocyanide/ferricyanide redox pair. The thermal-electrical conversion efficiency reached 2% ($\eta_{t/C}$ of 17%) when the cell was operated between 20 °C and 60 °C.[51] For long-term operation, the reduction in permselectivity of the ion-selective membrane could be an issue for this type of thermally-charged TREC.

The thermal-electrical efficiency (η_t) of a TREC is the ratio of the discharged electrical energy (W_e) and the required thermal energy (Q) for charging. The discharged electrical energy can be calculated as the difference between the maximum electrical energy (W_{max}) and the ohmic energy loss (W_{loss}), where W_{max} is the product of the differences in the low and high temperatures and the total entropy change in the cell reaction, or $W_{max} = \Delta T \Delta S$.[35,54] The ohmic energy loss can also be calculated as $W_{loss} = I(R_H + R_L)$, where I is the current used in cell discharging and charging (which are assumed to be equal), R_H the cell

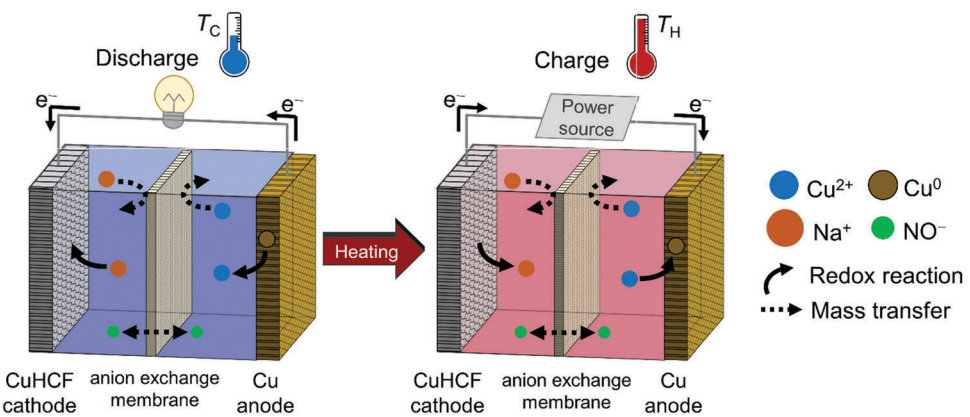

Fig. 3 Schematic of a TREC with a solid CuHCF cathode and a solid copper anode immersed in a copper nitrate (anolyte) and a sodium nitrate (catholyte) electrolyte, separated by an anion exchange membrane. The cell discharged at a low temperature (T_L) can be recharged at a higher temperature (T_H). The charging voltage at T_H is lower than that at T_L, leading to a net energy production by the voltage difference, which originated from the heat absorbed at the higher temperature.

internal resistance at T_H, and R_L the cell internal resistance at T_L. The thermal energy required for the cell charging includes the heat adsorption at T_H ($Q_H = T_H\Delta S$), and the external heat requirement to raise the temperature of the cell (Q_{HX}). Consequently, η_t can be expressed as[35]

$$\eta_t = \frac{W_e}{Q} = \frac{W_{max} - W_{loss}}{Q_H + Q_{HX}} = \frac{\Delta T\Delta S - I(R_H + R_L)nF}{T_H\Delta S + Q_{HX}} \quad (1)$$

The entropy change in the cell reaction of a TREC can be calculated as $\Delta S = \alpha_{cell}nF$, where α_{cell} is the temperature coefficient of the electrochemical cell (V/K), n is the number of electron transfer of the redox reaction, and F is the Faraday constant (96 485 C mol^{-1}), producing

$$\eta_t = \eta_C\frac{1 - I(R_H + R_L)/\alpha_{cell}\Delta T}{1 + \eta_C Q_{HX}/\alpha_{cell}nF\Delta T} \quad (2)$$

Using the Carnot efficiency, $\eta_C = 1 - T_L/T_H = \Delta T/T_H$, the thermal-electrical efficiency relative to the Carnot efficiency is therefore:

$$\eta_{t/C} = \frac{\eta_t}{\eta_C} = \frac{1 - I(R_H + R_L)/\alpha_{cell}\Delta T}{1 + \eta_C Q_{HX}/\alpha_{cell}nF\Delta T} \quad (3)$$

Power density is also a key parameter for evaluating conversion of low-grade heat to electricity. For a TREC, the average power production is[54]

$$P = \frac{(\alpha_{cell}\Delta T)^2}{8(R_H + R_L)} \quad (4)$$

These equations show the relationship between the low-grade heat temperature and thermal-electrical efficiency and power production.

2.3. Thermo-osmotic energy conversion

The concept of TOEC was recently introduced as an approach for generating electricity from low-grade heat.[34] In TOEC, a temperature difference is used to drive liquid through a membrane from a reservoir at ambient pressure to a high-pressure reservoir (Fig. 4). As thermo-osmotic (*i.e.*, temperature-driven) liquid flow occurs through the membrane, the liquid becomes pressurized. This flow is then depressurized through a turbine to do work and generate electricity. In principle, different liquids and membranes can be used in the system. Thus far, research has focused on systems utilizing water and hydrophobic porous membranes.[34,55] The hydrophobic membranes trap air within their pores when immersed in water forming a barrier between the two reservoirs (Fig. 4, inset). The temperature difference across the membrane causes a partial vapor pressure difference, which drives vapor flow from the hot to the cold side of the membrane.

Energy conversion in TOEC occurs because the membrane translates thermal energy to hydraulic energy. The maximum hydraulic pressure difference, ΔP_h, that can be theoretically generated with a given temperature difference in thermo-osmosis is defined by[56]

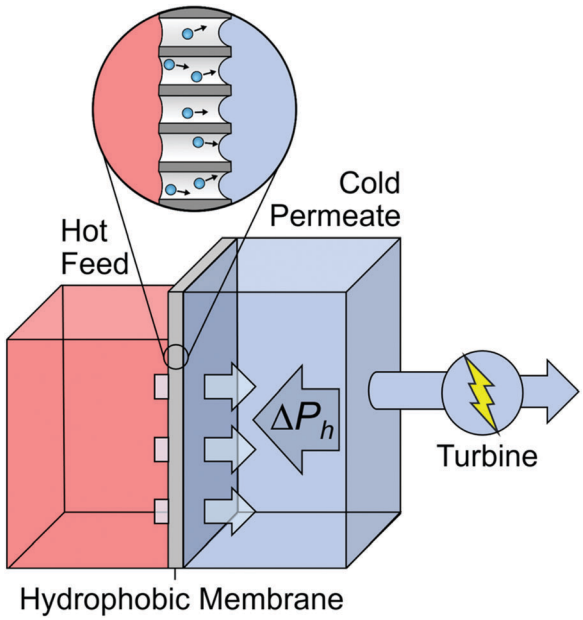

Fig. 4 Schematic of the TOEC process. A temperature difference across the membrane drives liquid from the hot feed to the cold permeate reservoir against a hydraulic pressure difference, ΔP_h. The pressurized flow of water is directed through a turbine to generate electricity. Inset shows water vapor transport through a hydrophobic porous membrane.

$$\Delta P_{h,max} = \frac{Q^*}{V_M}\left(1 - \frac{T_C}{T_H}\right) \quad (5)$$

where T_C is the temperature on the cold side of the membrane, T_H is the temperature on the hot side of the membrane, V_M is the molar volume of the liquid, and Q^* is the heat transferred per mole of fluid permeating across the membrane. For systems utilizing water and hydrophobic membranes, Q^* is equal to the enthalpy of vaporization of water (41 kJ mol^{-1}). Using this value of Q^*, the driving force from a given temperature difference is very large. For example, with only a 5 °C temperature difference across the membrane, the thermo-osmotic flow can theoretically generate hydraulic pressures up to around 40 MPa (400 bar).[34]

The first experimental demonstration of the TOEC system was conducted using water as working fluid and hydrophobic polytetrafluoroethylene (PTFE) membranes with a pore size around 77 nm.[34] The membrane operated up to a hydraulic pressure difference of 1.3 MPa (13 bar) before liquid water began displacing air in the membrane pores. Using a temperature of 60 °C in the hot feed reservoir and 20 °C in the cold permeate reservoir, a power density of 3.5 W m^{-2}-membrane was obtained at a hydraulic pressure difference of 1 MPa (10 bar).

The heat-to-electricity energy conversion efficiency of TOEC is highly dependent on how heat is managed in the system.[56] Heat transfer across the membrane will necessarily occur as water vapor evaporates on one side of the membrane and condenses on the other side, carrying with it the enthalpy of vaporization. However, there is also non-essential heat transfer

that occurs as heat is conducted in the membrane material and air gap. The thermal efficiency of the membrane, η_m, is used to quantify the effectiveness of heat transfer for a given membrane. This parameter is defined as the amount of heat transferred across the membrane in the enthalpy of vaporization divided by the total heat transferred.

$$\eta_m = \frac{J_w h_{vap}}{J_w h_{vap} + \frac{K_c}{\delta}\Delta T} \quad (6)$$

Here, J_w is the water flux across the membrane, h_{vap} is the enthalpy of vaporization, K_c is the thermal conductivity of the membrane, and δ is the thickness of the membrane. It is desirable to increase the thermal efficiency by enhancing the membrane permeability and reducing the thermal conductivity of the membrane.

Using a full-scale system analysis, the overall thermal-electrical efficiency, η_t, of TOEC can be obtained from the work output, W_e, divided by the thermal energy input, Q:[34]

$$\eta_t = \frac{W_e}{Q} = \frac{\Delta P_h \eta_m}{h_{vap}\rho}\left(\frac{\Delta T - \Delta T_{th,C} - \Delta T_M}{\Delta T_{th,H} + \Delta T_M + \Delta T_{HX}}\right) \quad (7)$$

where ρ is the density of the liquid, ΔT_M is the excess temperature difference in the membrane module, and ΔT_{HX} is the temperature difference in the heat exchanger. The thermal-electrical efficiency relative to the Carnot efficiency, $\eta_{t/C}$, can be obtained by dividing eqn (7) with the Carnot efficiency, $\eta_{t/C} = \eta_t/\eta_C$.

Lower values of ΔT_M and ΔT_{HX} represent more efficient systems with larger membrane modules and heat exchangers. In eqn (7), $\Delta T_{th,H}$ and $\Delta T_{th,C}$ are the threshold temperature differences on the hot and cold sides of the membrane module. These threshold temperature differences are needed to account for the impact of hydraulic pressure on the driving force across the membrane. They represent the effective loss in temperature difference across the membrane due to the applied hydraulic pressure difference, ΔP_h, and can be determined using eqn (5). Further explanation of the parameters used in the efficiency estimation is given elsewhere.[34,56]

Advanced models have been used to determine that the maximum efficiency of a realistic TOEC system will be around 34% of the Carnot efficiency (4.1% overall efficiency) when operated with hot and cold temperatures of 60 °C and 20 °C, respectively.[56] Obtaining this high efficiency will be possible if membranes are developed that can reach pressures of 50 bar, and if improvements that appear to be feasible are made in the membrane permeability. However, heat exchanger losses are also likely to reduce the obtainable efficiency by around 50%. Since TOEC is at the early stages of development, further experimental and theoretical studies will be needed to fully characterize the potential of this process for power production.

3. Power generation through regeneration of an external working fluid

An alternative approach to convert low-grade heat to electricity is to use the available heat in a working fluid regeneration unit instead of the power production unit. In this approach, the thermal energy can be stored for use until needed in an electrolyte as chemical energy and then converted into electrical power, enabling these technologies to both store energy and produce power when needed.

3.1. Technologies based on salinity gradients

Technologies have been developed to produce electricity from mixing two solutions of different concentrations or salinities.[36,57,58] While naturally occurring salinity gradients (*e.g.*, river water and seawater) have been widely investigated for power production, engineered salinity gradients generated by low-grade heat can also be used.[7,59–61] By using a thermally instable salt solution (*i.e.*, thermolytic solution) as the working fluid, such as ammonium bicarbonate, low-grade heat can be used in a conventional process such as a distillation column to separate ammonia and carbon dioxide, and generate streams with different salinities.[62–64] The practical efficiency of the process was estimated to be in the range of 5–10% of the Carnot efficiency.[63] Streams with different concentrations of ammonium bicarbonate (*i.e.*, working fluids) can then be used in a previously developed SGE-based process such as pressure retarded osmosis (PRO),[36,65–67] reverse electrodialysis (RED),[36,68,69] or capacitive mixing (CapMix).[70–73] SGE technologies with thermolytic solutions have several benefits when compared with seawater and river water, including no need of any chemical/physical pretreatment, and no constraints on location near rivers and seawater.[63,74] The power densities produced using ammonium bicarbonate solutions in RED have ranged from 0.20–0.84 W m^{-2}-membrane,[75–78] and from 5–10 W m^{-2}-membrane using PRO.[79,80] Maximum power densities using CapMix have been significantly lower, with 6.3 mW m^{-2} produced using manganese oxide and metallic lead electrodes.[81]

3.2. Thermally regenerative batteries

A new approach developed in 2015 for producing electricity, called a thermally regenerative battery (TRB), is based on oxidation and reduction of metal electrodes.[37] In a TRB, chemical potential is generated from the formation of metal ammine complexes, which are produced by adding a ligand such as ammonia to one electrolyte making it the anolyte, but not to the other electrolyte (catholyte). When the potential difference between the electrodes is discharged, the anode undergoes oxidative dissolution, and aqueous metal ions are reduced and deposited on the cathode. After the cell discharges, the ligand is separated from the anolyte using a conventional heat-based separation technology, such as distillation, and then added to the other electrolyte for the next discharge cycle. The first developed TRB used copper electrodes and ammonia as the ligand in the anolyte (a thermally regenerative ammonia battery, TRAB). A copper nitrate salt with an ammonium nitrate as the supporting electrolyte was used in both chambers (Fig. 5).[37,82]

TRBs have already produced significantly higher power densities than the previous thermal-electrical conversion approaches. The first TRAB using ammonia as the ligand produced a maximum power density of $P = \sim 80$ W m^{-2}-electrode area, with a thermal efficiency relative to the Carnot efficiency of $\eta_{t/C} = 6.2\%$.[37] Both power density and thermal-electrical efficiency were improved

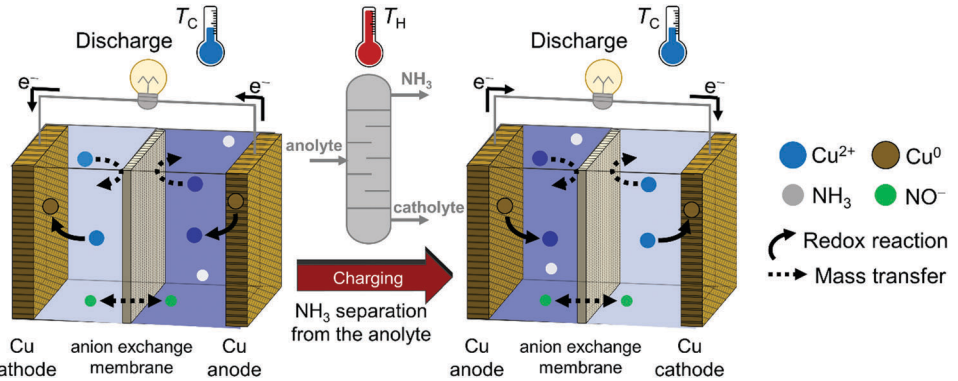

Fig. 5 Schematic of a TRB with copper electrodes and copper salts as well as ammonia only in the anolyte. Two chambers are separated by an anion exchange membrane. After the cell discharges at room temperature, ammonia is separated from the anolyte using a conventional distillation process, and then added to the other electrolyte for the sequel discharge cycle. Unlike TEC in which power is produced as long as a temperature gradient is present inside the cell, TREC and TRB generate electricity in a cell with a constant temperature and utilize thermal energy to recharge the cell, enabling the system to store energy (*i.e.*, performing as a battery).

using an anion exchange membrane with lower resistance, producing P = 106 W m^{-2} with $\eta_{t/C}$ = 7%.[83] By using ethylenediamine as the ligand in a TRB, called a thermally regenerative ethylenediamine battery (TRENB), power was further increased to 120 W m^{-2}, which was 1.5 times higher that of a TRAB.[84] However, because ethylenediamine is an azeotrope, its separation from solution was estimated to require more energy than that of an ammonia solution, and so the thermal efficiency relative to the Carnot efficiency was lower, at $\eta_{t/C}$ = 3.1%. Energy recoveries could likely be improved for all these TRB processes through optimization of the separation processes.

TRB performance can be improved through the use of elevated temperatures. For example, a TRAB showed a linear increase in maximum power densities with temperature, producing 236 W m^{-2} (normalized to the projected electrode area) at 72 °C, compared to 95 W m^{-2} at 23 °C.[82] This was the highest power density reported for a low-grade heat conversion system. A high $\eta_{t/C}$ of 12.5% was also obtained at 72 °C.[82] The improved power at higher temperatures was due to reduced electrode overpotentials and more favorable thermodynamics for the reactions, particularly copper oxidation at the anode. However, operation at higher temperatures increased self-discharge as a result of reduced membrane selectivity, due to ammonia transport across the anion exchange membrane, which resulted in a decrease in energy densities.

The main challenge of electricity production using TRABs is long-term stability of the electrodes over multiple cycles. TRABs based on copper electrodes could only be operated for a limited number of recharging cycles due to unbalanced rates of gain and loss of metal on the copper electrodes (*i.e.*, low reversibility). While the cathodic deposition of copper is efficiently regained from the current (*i.e.*, good cathodic coulombic efficiency, CCE), the conversion of anode copper into current of TRABs is only 35% (*i.e.*, anodic coulombic efficiency, ACE).[37,82,85] The use of ethylenediamine (TRENB) as an alternative ligand to ammonia (TRAB) enhanced the ACE to 77%.[84] Despite this significant improvement in ACE by using ethylenediamine instead of ammonia, irreversible losses of copper from the anode were not eliminated. To address the reversibility issue, a silver-based TRAB with an ammonia ligand (Ag-TRAB) and carbon electrodes was proposed as an alternative to the copper-based TRAB.[86] With silver, the cathodic and anodic coulombic efficiencies of the TRAB were the same (~100%), resulting in a fully reversible system for converting low-grade heat into electricity over many successive cycles. Successive deposition and dissolution cycling showed the system was stable over a hundred cycles. While the cost of Ag is much higher than that of copper, the mass of Ag used in the Ag-TRAB was minimized by using carbon electrodes and silver salt solutions rather than solid or mesh metal electrodes used for the copper TRAB.

Both fed-batch and flow reactor configurations have been examined for electricity production using TRABs. The first TRAB configuration was a small fed-batch reactor, with relatively large catholyte and anolyte chambers compared to the size of the copper mesh electrodes, producing an overall electrode area per volume of reactor of 6 m^2 m^{-3}.[37,87] The 1 cm distance between the electrodes also contributed to a high proportion of the total internal resistance due to the solution resistance. For example, in this fed-batch cell with 0.1 M copper nitrate, 5 M ammonium nitrate and 2 M ammonia, the solution resistance was 22% of the total resistance of the cell.[37] To improve the electrode specific area and decrease the cell resistance, more compact flow configurations were developed for copper and silver-based TRABs.[85,86] The electrode surface area per volume was increased from 6 m^2 m^{-3} (fed-batch) to 600 m^2 m^{-3} (flow Cu-TRAB) or 10 000 m^2 m^{-3} (flow Ag-TRAB), resulting in higher energy densities. For example, the energy density of a flow Cu-TRAB increased by up to 40% compared to that of the fed-batch Cu-TRAB.[85] The power density of flow TRABs could be further improved by simply stacking individual cells in series or parallel configurations. The result showed that P of a Cu-TRAB linearly increases with the number of cell pairs, with a slope of 16 mW per cell pair.[85]

Thermal-electrical energy conversion in TRBs is a two-step process: low-grade heat is first converted to the chemical energy stored in the battery during the charge process, and then the chemical energy is converted to electrical power during the

discharge process.[37,84] The charging energy efficiency (η_{ch}) is calculated as the ratio between the chemical energy stored in the battery (ΔG) and the required thermal energy (Q) for electrolyte regeneration (*i.e.*, battery charging), as:

$$\eta_{ch} = \frac{\Delta G}{Q} = \frac{-nFE_{OCV}}{Q} \quad (8)$$

where E_{OCV} is the cell open-circuit voltage. The discharge energy efficiency (η_d) is the ratio of the discharged electrical energy (W_e) and the chemical energy stored in the battery, or[86]

$$\eta_d = \frac{W_e}{-nFE_{OCV}} = \frac{\int P dt}{-nFE_{OCV}} \quad (9)$$

where the discharged electrical energy is calculated by integrating the power-time profile.

The overall thermal energy efficiency (η_t) is then defined to determine the efficiency of TRB for converting low-grade heat to electricity, and is calculated as the ratio of the discharged electrical energy and the thermal energy required for the battery charge, as:

$$\eta_t = \frac{\int P dt}{Q} \quad (10)$$

To provide a better comparison between TRBs and other techniques, the overall thermal energy can be compared to the Carnot efficiency (η_C). The thermal efficiency relative to the Carnot efficiency is therefore:

$$\eta_{t/C} = \frac{\eta_t}{\eta_C} = \frac{\int P dt}{Q\left(1 - \frac{T_L}{T_H}\right)} \quad (11)$$

This last result shows the direct relationship between electrical power production and the low-grade heat temperature.

4. Prospects for low-grade heat conversion to electricity using liquid-based technologies

The conversion of low-grade heat into electrical power using liquid-based technologies offers many advantages over the solid-state thermoelectrics, including higher power densities and conversion efficiencies, the use of inexpensive materials, and the possibility of energy storage. A comparison of the representative higher power densities and efficiencies for the seven different thermally-based processes, the relatively newer technologies, TOEC, TREC, and TRB, exhibit higher power densities and energy conversion efficiencies than older technologies (Fig. 6a). Considering these three technologies are also quite recently developed compared to the other processes (Fig. 6b), they may have a greater potential for further improvement compared to other processes that have been under development for decades. The older technologies have improved in terms of power densities and thermal efficiencies, but in general they lag behind those produced with the newer technologies. For example, the highest P reported for a TEC of 12 W m^{-2} was an order of magnitude lower than those of TRBs

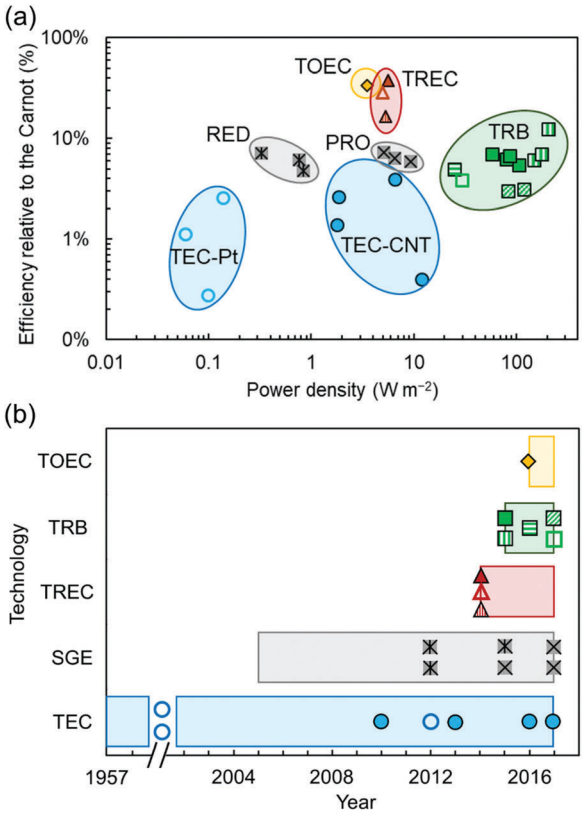

Fig. 6 Comparison of the liquid-based approaches of converting low-grade heat to electricity. The figure indicates (a) the power density and efficiency relative to the Carnot limit and (b) research time of TEC (blue colored) with platinum (TEC-Pt, open symbols)[39] or with carbon nanotube electrodes (TEC-CNT, filled symbols);[31,40,42,49] SGE (gray colored) technologies including RED (asterisk),[75–78] and PRO (cross);[79,80] TREC (red colored) with (filled symbol),[35] or without (open symbol)[52] an ion-exchange membrane, or a charging-free TREC (patterned symbol);[51] TRB (green colored) with a batch reactor and copper electrodes and ammonia ligand at room (filled symbols)[37,83] or elevated (vertical line) temperatures,[82] a TRB with ethylene-diamine ligand (diagonal line),[84] and a flow copper (horizontal line)[85] or silver (open symbol) TRB;[86] and TOEC (orange colored).[34,56] The highlighted area in part b indicates the time period that each technology has been developed. The power densities reported here are for lab-scale systems with relatively small electrode or/and membrane areas.

($P \sim 100$ W m^{-2}). Future applications of TECs are envisioned to be focused more on designing this technology as wearable devices for power production, where the utilization of body heat could power small portable electronics that require very low power densities, rather than for large-scale electricity generation.

To bring TOEC, TREC and TRB technologies to practical applications at larger scales, improvements are still needed to enhance the power densities and/or conversion efficiencies, while further reducing the cost of materials. For example, to make TRECs more competitive, power densities in particular would need to be improved, as they are only ~5 W m^{-2}-electrode area.[37] The improvement in power density could be obtained through optimizing the cell configuration and the salt concentrations, using electrodes with faster charge transfer kinetics, and by decreasing a cell's internal resistance. For example, membranes with lower resistances could be fabricated, and electrolytes with

higher conductivities could be used. The electrode reversibility and cell durability are particularly important for TRECs. In TRECs that use a copper anode, the rate of copper dissolution during the cell discharge and the rate of deposition during the charging process should be carefully monitored. An unbalanced rate of dissolution and deposition leads to a loss of copper from the electrode, which would impair long-term operation. In addition, the durability of the cell materials, especially the membranes, should be considered in future studies.

To advance TOEC systems, further experimental work is needed to demonstrate that increased power densities can be obtained by using higher pressures, which would shift this technology in Fig. 6 toward the top right of the plot. To achieve this goal, hydrophobic porous membranes must be produced that are able to withstand hydraulic pressures of at least 50 bar by decreasing the membrane pore size and increasing hydrophobicity.[34] Improvements in membrane structure to increase permeability and porosity will also aid in enhancing performance. These improvements should be feasible given recent advances in membranes for other applications such as membrane distillation.[88–90] The TOEC efficiency may also benefit from using working fluids in closed-loop cycles with a lower heat of vaporization (*e.g.*, organic solvents) or by optimizing the process to improve heat recovery.[34,55]

A variety of challenges remain to improve the performance and sustainability of TRBs for producing electricity using low-grade heat sources. For TRBs, power densities are the highest of all these technologies, but the heat-to-electricity efficiency of TRBs needs to be improved through optimization of the charging process. To date, all estimates of thermal efficiencies are based on process simulations using only a partially optimized approach with a vacuum distillation column and not actual systems. The heat duty was estimated by optimizing temperature, pressure, and molar flow,[37,82,85] but the thermal energy requirements could be further improved by optimizing other distillation column parameters including the number of stages, feed stage location, and reflux ratio. Alternative separation processes could also be explored, such as air stripping, to decrease the separation energy requirements, and thus, improve the overall thermal-electrical conversion efficiency. Higher power densities could likely be obtained using Ag-TRABs, as the impact of temperature has so far only been examined for copper-based TRABs (Cu-TRABs).[82] A stack of flow Ag-TRABs connected in parallel or series could also likely improve power and energy densities as shown for Cu-TRABs. The power densities of TRBs have only been reported for lab-scale cells with relatively small electrode areas. In order to have a more accurate estimation of power density, a scaled up TRB should be built and operated.

A more comprehensive techno-economic analysis is needed to better evaluate the extent that specific advances are needed for these various technologies (TOEC, TREC, or TRB) to make them competitive with electricity generation using other technologies. An initial economic analysis for a Ag-TRAB system based on just the materials showed that materials costs were 1.8 times more than the average electricity price in the U.S. ($120 MW h^{-1}), due primarily to the cost of the membrane and the silver.[86] However, it was estimated that this could be reduced to $120 MW h^{-1} if the cost of just the membranes was reduced to $10 m^{-2}. Such a reduction of membrane costs could likely be achieved through mass production of the membranes, as shown by the large decrease in reverse osmosis membrane cost as the technology has achieved much greater market penetration in the seawater desalination field. Other potential benefits of these new low heat technologies, such as a lack of air pollution for the electricity produced, and beneficial issues related to health and climate change, should also be included in a full life-cycle analysis. Although the costs of building and operating these low-grade heat conversion technologies are currently higher than that of conventional technologies, such approaches could provide a clean method of electrical power generation from resources that are currently not captured for this purpose.

Conflicts of interest

There are no conflicts to declare.

Acknowledgements

The research was supported by the National Science Foundation (NSF) through awards CBET-1464891 and CBET-1603635, and funding from Penn State University.

References

1 L. E. Bell, *Science*, 2008, **321**, 1457–1461.
2 S. Chu and A. Majumdar, *Nature*, 2012, **488**, 294–303.
3 S. Tavakkoli, O. R. Lokare, R. D. Vidic and V. Khanna, *ACS Sustainable Chem. Eng.*, 2016, **4**, 3618–3626.
4 I. Johnson, W. T. Choate and A. Davidson, *Waste heat recovery. Technology and opportunities in US industry*, BCS, Inc., Laurel, MD, United States, 2008.
5 M. H. Dickson and M. Fanelli, *Geothermal energy: utilization and technology*, Taylor & Francis, 2013.
6 *International Energy Agency*, 2016, https://www.iea.org/publications/freepublications/publication/WorldEnergyOutlook2016ExecutiveSummaryEnglish.pdf.
7 N. Y. Yip, D. Brogioli, H. V. M. Hamelers and K. Nijmeijer, *Environ. Sci. Technol.*, 2016, **50**, 12072–12094.
8 *International Energy Agency Energy policies of IEA countries The United States 2014 review*, 2014, vol. 40, https://www.iea.org/publications/freepublications/publication/USA_2014.pdf.
9 D. B. Gingerich and M. S. Mauter, *Environ. Sci. Technol.*, 2015, **49**, 8297–8306.
10 H. Lu, L. Price and Q. Zhang, *Appl. Energy*, 2016, **161**, 497–511.
11 R. Law, A. Harvey and D. Reay, *Appl. Therm. Eng.*, 2013, **53**, 188–196.
12 O. R. Lokare, S. Tavakkoli, G. Rodriguez, V. Khanna and R. D. Vidic, *Desalination*, 2017, **413**, 144–153.
13 S. B. Riffat and X. L. Ma, *Appl. Therm. Eng.*, 2003, **23**, 913–935.
14 P. J. Mago, L. M. Chamra, K. Srinivasan and C. Somayaji, *Appl. Therm. Eng.*, 2008, **28**, 998–1007.

15 A. Uusitalo, J. Honkatukia and T. Turunen-Saaresti, *Appl. Energy*, 2017, **192**, 146–158.
16 W. C. Xu, J. Y. Zhang, L. Zhao, S. Deng and Y. Zhang, *Energy Convers. Manage.*, 2017, **137**, 1–11.
17 T. J. Salez, B. T. Huang, M. Rietjens, M. Bonetti, C. Wiertel-Gasquet, M. Roger, C. L. Filomeno, E. Dubois, R. Perzynski and S. Nakamae, *Phys. Chem. Chem. Phys.*, 2017, **19**, 9409–9416.
18 H. Chen, D. Y. Goswami and E. K. Stefanakos, *Renewable Sustainable Energy Rev.*, 2010, **14**, 3059–3067.
19 L. Jing, P. Gang and J. Jie, *Appl. Energy*, 2010, **87**, 3355–3365.
20 L. Tocci, T. Pal, I. Pesmazoglou and B. Franchetti, *Energies*, 2017, **10**, 26.
21 S. Quoilin, M. Van den Broek, S. Declaye, P. Dewallef and V. Lemort, *Renewable Sustainable Energy Rev.*, 2013, **22**, 168–186.
22 J. Bao and L. Zhao, *Renewable Sustainable Energy Rev.*, 2013, **24**, 325–342.
23 K. Biswas, J. He, I. D. Blum, C.-I. Wu, T. P. Hogan, D. N. Seidman, V. P. Dravid and M. G. Kanatzidis, *Nature*, 2012, **489**, 414–418.
24 S. B. Riffat and X. Ma, *Appl. Therm. Eng.*, 2003, **23**, 913–935.
25 O. Bubnova and X. Crispin, *Energy Environ. Sci.*, 2012, **5**, 9345–9362.
26 M. Zebarjadi, K. Esfarjani, M. S. Dresselhaus, Z. F. Ren and G. Chen, *Energy Environ. Sci.*, 2012, **5**, 5147–5162.
27 J. He and T. M. Tritt, *Science*, 2017, **357**, eaak9997.
28 A. R. M. Siddique, S. Mahmud and B. V. Heyst, *Renewable Sustainable Energy Rev.*, 2017, **73**, 730–744.
29 T. Mancini, P. Heller, B. Butler, B. Osborn, W. Schiel, V. Goldberg, R. Buck, R. Diver, C. Andraka and J. Moreno, *J. Sol. Energy Eng.*, 2003, **125**, 135–151.
30 C. B. Vining, *Nat. Mater.*, 2009, **8**, 83–85.
31 R. Hu, B. A. Cola, N. Haram, J. N. Barisci, S. Lee, S. Stoughton, G. Wallace, C. Too, M. Thomas, A. Gestos, M. E. D. Cruz, J. P. Ferraris, A. A. Zakhidov and R. H. Baughman, *Nano Lett.*, 2010, **10**, 838–846.
32 T. J. Abraham, D. R. MacFarlane and J. M. Pringle, *Chem. Commun.*, 2011, **47**, 6260–6262.
33 M. Dupont, D. MacFarlane and J. Pringle, *Chem. Commun.*, 2017, **53**, 6288–6302.
34 A. P. Straub, N. Y. Yip, S. Lin, J. Lee and M. Elimelech, *Nat. Energy*, 2016, **1**, 16090.
35 S. W. Lee, Y. Yang, H.-W. Lee, H. Ghasemi, D. Kraemer, G. Chen and Y. Cui, *Nat. Commun.*, 2014, 5.
36 B. E. Logan and M. Elimelech, *Nature*, 2012, **488**, 313–319.
37 F. Zhang, J. Liu, W. Yang and B. E. Logan, *Energy Environ. Sci.*, 2015, **8**, 343–349.
38 A. Gunawan, C.-H. Lin, D. A. Buttry, V. Mujica, R. A. Taylor, R. S. Prasher and P. E. Phelan, *Nanoscale Microscale Thermophys. Eng.*, 2013, **17**, 304–323.
39 U. B. Holeschovsky, *Analysis of flooded flow fuel cells and thermogalvanic generators*, Massachusetts Institute of Technology, 1994.
40 M. S. Romano, N. Li, D. Antiohos, J. M. Razal, A. Nattestad, S. Beirne, S. Fang, Y. Chen, R. Jalili, G. G. Wallace, R. Baughman and J. Chen, *Adv. Mater.*, 2013, **25**, 6602–6606.
41 N. E. Holubowitch, J. Landon, C. A. Lippert, J. D. Craddock, M. C. Weisenberger and K. Liu, *ACS Appl. Mater. Interfaces*, 2016, **8**, 22159–22167.
42 H. Im, T. Kim, H. Song, J. Choi, J. S. Park, R. Ovalle-Robles, H. D. Yang, K. D. Kihm, R. H. Baughman, H. H. Lee, T. J. Kang and Y. H. Kim, *Nat. Commun.*, 2016, 7.
43 J. He, D. Al-Masri, D. R. MacFarlane and J. M. Pringle, *Faraday Discuss.*, 2016, **190**, 205–218.
44 M. A. Lazar, D. Al-Masri, D. R. MacFarlane and J. M. Pringle, *Phys. Chem. Chem. Phys.*, 2016, **18**, 1404–1410.
45 T. Kim, J. S. Lee, G. Lee, H. Yoon, J. Yoon, T. J. Kang and Y. H. Kim, *Nano Energy*, 2017, **31**, 160–167.
46 P. F. Salazar, S. Kumar and B. A. Cola, *J. Appl. Electrochem.*, 2013, **44**, 325–336.
47 J. N. Agar and W. G. Breck, *Trans. Faraday Soc.*, 1957, **53**, 167–178.
48 Y. Mua and T. I. Quickenden, *J. Electrochem. Soc.*, 1996, **143**, 2558–2564.
49 L. Zhang, T. Kim, N. Li, T. J. Kang, J. Chen, J. M. Pringle, M. Zhang, A. H. Kazim, S. Fang, C. Haines, D. Al-Masri, B. A. Cola, J. M. Razal, J. Di, S. Beirne, D. R. MacFarlane, A. Gonzalez-Martin, S. Mathew, Y. H. Kim, G. Wallace and R. H. Baughman, *Adv. Mater.*, 2017, **29**, 1605652.
50 H. L. Chum and R. A. Osteryoung, *Review of thermally regenerative electrochemical systems*, Solar Energy Research Inst., Golden, CO, USA, State Univ. of New York, Buffalo, USA, 1981.
51 Y. Yang, S. W. Lee, H. Ghasemi, J. Loomis, X. Li, D. Kraemer, G. Zheng, Y. Cui and G. Chen, *Proc. Natl. Acad. Sci. U. S. A.*, 2014, **111**, 17011–17016.
52 Y. Yang, J. Loomis, H. Ghasemi, S. W. Lee, Y. J. Wang, Y. Cui and G. Chen, *Nano Lett.*, 2014, **14**, 6578–6583.
53 J. R. Varcoe, P. Atanassov, D. R. Dekel, A. M. Herring, M. A. Hickner, P. A. Kohl, A. R. Kucernak, W. E. Mustain, K. Nijmeijer, K. Scott, T. Xu and L. Zhuang, *Energy Environ. Sci.*, 2014, **7**, 3135–3191.
54 C. Gao, S. W. Lee and Y. Yang, *ACS Energy Lett.*, 2017, **2**, 2326–2334.
55 W. A. Phillip, *Nat. Energy*, 2016, **1**, 16101.
56 A. P. Straub and M. Elimelech, *Environ. Sci. Technol.*, 2017, **51**, 12925–12937.
57 G. Z. Ramon, B. J. Feinberg and E. M. Hoek, *Energy Environ. Sci.*, 2011, **4**, 4423–4434.
58 A. D'Angelo, M. Tedesco, A. Cipollina, A. Galia, G. Micale and O. Scialdone, *Water Res.*, 2017, **125**, 123–131.
59 V. G. Gude, *Appl. Energy*, 2015, **137**, 877–898.
60 A. Carati, M. Marino and D. Brogioli, *Energy*, 2015, **93**, 984–993.
61 K. L. Hickenbottom, J. Vanneste, L. Miller-Robbie, A. Deshmukh, M. Elimelech, M. B. Heeley and T. Y. Cath, *J. Membr. Sci.*, 2017, **535**, 178–187.
62 J. R. McCutcheon, R. L. McGinnis and M. Elimelech, *Desalination*, 2005, **174**, 1–11.
63 R. L. McGinnis, J. R. McCutcheon and M. Elimelech, *J. Membr. Sci.*, 2007, **305**, 13–19.
64 S. Lin, N. Y. Yip, T. Y. Cath, C. O. Osuji and M. Elimelech, *Environ. Sci. Technol.*, 2014, **48**, 5306–5313.
65 J. W. Post, J. Veerman, H. V. Hamelers, G. J. Euverink, S. J. Metz, K. Nymeijer and C. J. Buisman, *J. Membr. Sci.*, 2007, **288**, 218–230.

66 H. W. Chung, L. D. Banchik and J. Swaminathan, *Desalination*, 2017, **408**, 133–144.
67 E. Shaulsky, C. Boo, S. Lin and M. Elimelech, *Environ. Sci. Technol.*, 2015, **49**, 5820–5827.
68 M. Tedesco, A. Cipollina, A. Tamburini, I. D. L. Bogle and G. Micale, *Chem. Eng. Res. Des.*, 2015, **93**, 441–456.
69 X. Zhu, T. Kim, M. Rahimi, C. A. Gorski and B. E. Logan, *ChemSusChem*, 2017, **10**, 797–803.
70 D. Brogioli, R. Ziano, R. Rica, D. Salerno, O. Kozynchenko, H. Hamelers and F. Mantegazza, *Energy Environ. Sci.*, 2012, **5**, 9870–9880.
71 T. Kim, M. Rahimi, B. E. Logan and C. A. Gorski, *Environ. Sci. Technol.*, 2016, **50**, 9791–9797.
72 F. Liu, O. Schaetzle, B. B. Sales, M. Saakes, C. J. Buisman and H. V. Hamelers, *Energy Environ. Sci.*, 2012, **5**, 8642–8650.
73 C. Lian, C. Zhan, D.-E. Jiang, H. Liu and J. Wu, *J. Phys. Chem. C*, 2017, **121**, 14010–14018.
74 R. D. Cusick, Y. Kim and B. E. Logan, *Science*, 2012, **335**, 1474–1477.
75 X. Luo, X. Cao, Y. Mo, K. Xiao, X. Zhang, P. Liang and X. Huang, *Electrochem. Commun.*, 2012, **19**, 25–28.
76 K. Kwon, B. H. Park, D. H. Kim and D. Kim, *Energy Convers. Manage.*, 2015, **103**, 104–110.
77 X. Zhu, W. He and B. E. Logan, *J. Membr. Sci.*, 2015, **494**, 154–160.
78 D. H. Kim, B. H. Park, K. Kwon, L. Li and D. Kim, *Appl. Energy*, 2017, **189**, 201–210.
79 A. Altaee, P. Palenzuela, G. Zaragoza and A. A. AlAnezi, *Appl. Energy*, 2017, **191**, 328–345.
80 D. D. Anastasio, J. T. Arena, E. A. Cole and J. R. McCutcheon, *J. Membr. Sci.*, 2015, **479**, 240–245.
81 T. Kim, M. Rahimi, B. E. Logan and C. A. Gorski, *ChemSusChem*, 2016, **9**, 981–988.
82 F. Zhang, N. LaBarge, W. Yang, J. Liu and B. E. Logan, *ChemSusChem*, 2015, **8**, 1043–1048.
83 M. Rahimi, L. Zhu, K. L. Kowalski, X. Zhu, C. A. Gorski, M. A. Hickner and B. E. Logan, *J. Power Sources*, 2017, **342**, 956–963.
84 M. Rahimi, A. D'Angelo, C. A. Gorski, O. Scialdone and B. E. Logan, *J. Power Sources*, 2017, **351**, 45–50.
85 X. Zhu, M. Rahimi, C. A. Gorski and B. Logan, *ChemSusChem*, 2016, **9**, 873–879.
86 M. Rahimi, T. Kim, C. A. Gorski and B. E. Logan, *J. Power Sources*, 2018, **373**, 95–102.
87 M. Rahimi, Z. Schoener, X. Zhu, F. Zhang, C. A. Gorski and B. E. Logan, *J. Hazard. Mater.*, 2017, **322**, 551–556.
88 J. Lee, T. Laoui and R. Karnik, *Nat. Nanotechnol.*, 2014, **9**, 317–323.
89 Y. Zhang, J. L. Sargent, B. W. Boudouris and W. A. Phillip, *J. Appl. Polym. Sci.*, 2015, 132.
90 E. Shaulsky, S. Nejati, C. Boo, F. Perreault, C. O. Osuji and M. Elimelech, *J. Membr. Sci.*, 2017, **530**, 158–165.